Finite element analysis of Bridge Crane Metal Structure Based on ABAQUS

Zhong Meng[1], Tong Yifei [1] and LI Xiangdong [2]

[1]*Nanjing University of Science and Technology, Nanjing, China*
[2]*Jiangsu Province Special Equipment Safety Supervision Inspection Institute, Nanjing, China*

Abstract. Taking the QD-type (50/10t-31.5) bridge crane as the research object and the finite element method as theoretical basis, the metal structure using ABAQUS software is analyzed. Firstly, the three-dimensional model of the metal structure is established according to the design parameters. Second, the bridge crane under three typical operation conditions is analyzed and the stress and displacement analysis results are presented. And, the strength and stiffness of the crane are verified based on the analysis results. Moreover, the maximum stress and displacement under dangerous conditions of the crane are calculated by theoretical calculation. By comparing the results of the theoretical method and the finite element method. The research can favor to increase the design efficiency.

1 Introduction

With the continuous development of the crane industry, the demand for design quality has increased [1]. In order to reduce the design cost, an effective design method is inevitably required. Traditional method is for engineers to estimate the strength at the initial stage of design [2]. Although it is safe and reliable, it will cause waste of resources due to the high safety factor. The modern design generally uses the finite element method as the theoretical basis to comprehensively use CAE analysis software to analyze the structure of the crane [3]. The analysis process of finite element method can be summarized as: discretization of continuum, unit analysis, global analysis, constraint conditions determination, solution to finite element equations, and analysis and discussion of results [4]. The key to this analysis method is to establish a reasonable and effective model. This article provides a more accurate analysis for the static structural analysis of the bridge crane metal structure.

2 The FEA modeling of metal structure

2.1 Three-dimensional modeling

As the main bearing component, the metal structure of the bridge crane is composed of the main girder, end beam and trolley rail. The metal structure of crane is shown in Fig 1[5].

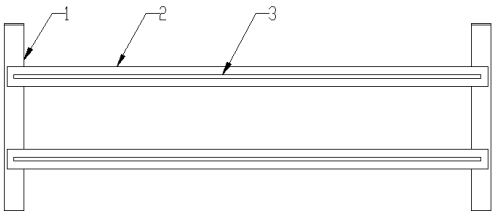

1. End beam 2. Main girder 3. Trolley rail
Figure 1. Metal structure of the crane.

The establishment of the three-dimensional finite element model is the basis for structural analysis. The accuracy of the model directly affects the analysis results. Select the shell element model according to the structural characteristics of the welded box beam, and the minimum aspect ratio a=371/8=46.25>10 in all steel plates. Firstly, using ABAQUS/CAE module to establish the three parts of the rail, main girder and end beam [6]. Then using Assembly module to obtain a three-dimensional finite element model. In order to improve the analysis efficiency, the model can be simplified, such as removing fillets, small holes, etc. Three-dimensional model is shown in Fig 2

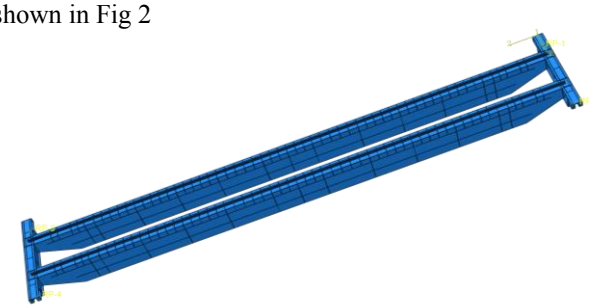

Figure 2. Overall 3D model of the metal structur

2.2 Setting material

The girder is welded using Q235 steel plate. The main mechanical properties of the material are shown in Table 1.

Table 1. Material properties of the girder.

Type	Young's Modulus (GPa)	Poisson's Ratio	Density (g/cm^3)	Tensile Strength (MPa)	Yield Strength (MPa)
Q235	210	0.3	785	375	235

2.3 Interactions definition

The analysis model is assembled from the main girder, end beam and trolley rail. The contact between the cover plate of main girder and the lower surface of the rail has little impact on the entire model and is always in close contact with the entire analysis process. Therefore, use Tie to define the relationship between them. This relationship not only eliminates rigid body displacement of the model, but also greatly reduces the iterations for calculation of the contact state. Set the position tolerance as 0.01 to eliminate contact surface gap due to dimensional deviation.

2.4 Loads definition

This paper analyzes the stress and displacement of the structure under three working conditions: fully loaded travelling crab is located in the middle of the girder, 1/4 and the end of the girder. According to the actual working conditions, the structure can be treated as simply supported beam. Fig 3 shows the loads of the girder when the travelling crab is in the middle, where G is the evenly distributed weight of the structure , Q1 and Q2 are the concentrated loads caused by the lifting weights at the two wheels, and P is the weight of the travelling crab.

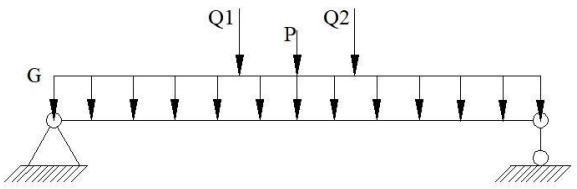

Figure 3. Load condition of the girder.

Gravity load. Simply set the material density $\rho = 7.85E-9 t/mm^3$ and gravitational acceleration $g = 9800\phi_1 = 10780\,mm/s^2$ in Abaqus software. Introduce hoisting impact factor $\phi_1 = 1.1$ to take into account the influence of crane's own weight vibration load.

Working load. The weight of travelling crab P=153860N, and lifting load Q=490000N. Average working load on four wheels of the travelling crab and get $F = \frac{P + Q\phi_2}{4} = 178115N$, where the lifting dynamic load factor $\phi_2 = 1.15$ is set to take into account the dynamic effect of the increased load due to inertial forces.

2.5 Boundary conditions

Set the reference points at the wheel center of the end beam, and couple these points to the end faces of the beam, as shown in Fig 4 The boundary condition is imposed on reference points: constrained movement of the x, y, z direction and rotational freedom in the x, z direction of one fixed end; and at another hinged end, constrained movement in the y, z direction and rotational freedom in the x, z direction. The reference points are shown in Fig 5.

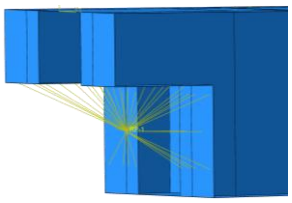

Figure 4. End faces of the beam.

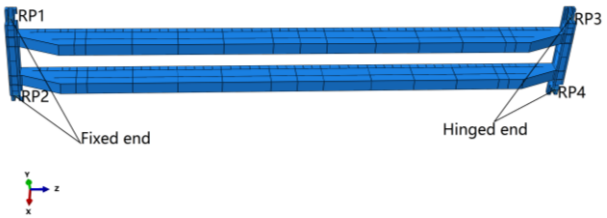

Figure 5. Location of reference point.

2.6 Mesh

The part rail is a three-dimensional solid model, for which the seeds with an approximate global size of 50 are arranged, the hexahedral grid is divided by the sweep technology, and the cell type is C3D8R (linear reduction of the eight-node three-dimensional solids). The mesh is verified without errors or warnings. The main girder is a shell element model, for which the seeds with an approximate global size of 50 are arranged. The free technology is used to divide the quadrilateral mesh. The element type is S4R (linear reduction of the four-node shell). There are three highlight warnings in the model. Solve these problems through geometric clean function module. The mesh of end beam is set in the same way as the main girder.

The pre-processing of the finite element analysis has been completed, and next, the model will be submitted to the module of Abaqus/Standard for calculation.

3 Analysis result

The stress nephogram when the travelling crab is fully loaded in the middle of the girder is shown in Fig 6, and Fig 7 shows the displacement nephogram of trolley with full loaded in 1/2 cross girder.The results of finite element calculations show that the maximum stress and displacement and their main hotspot areas of the crane metal structure under three typical operating conditions are shown in Table 2.

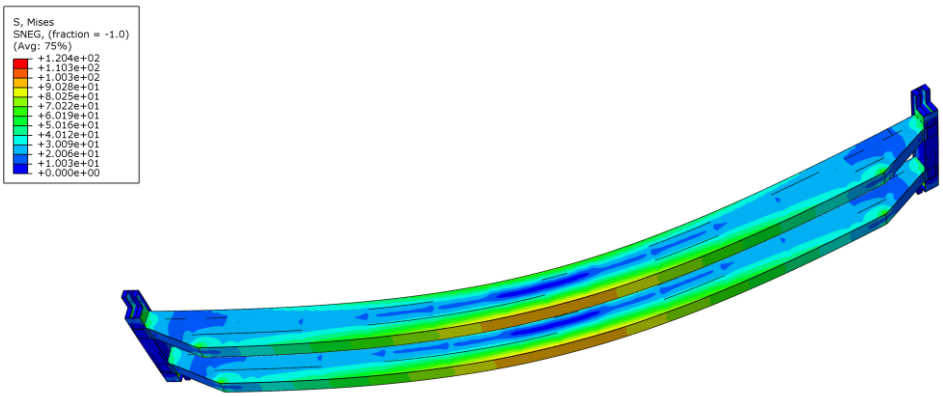

Figure 6. Equivalent stress nephogram of trolley with full loaded in 1/2 cross girder.

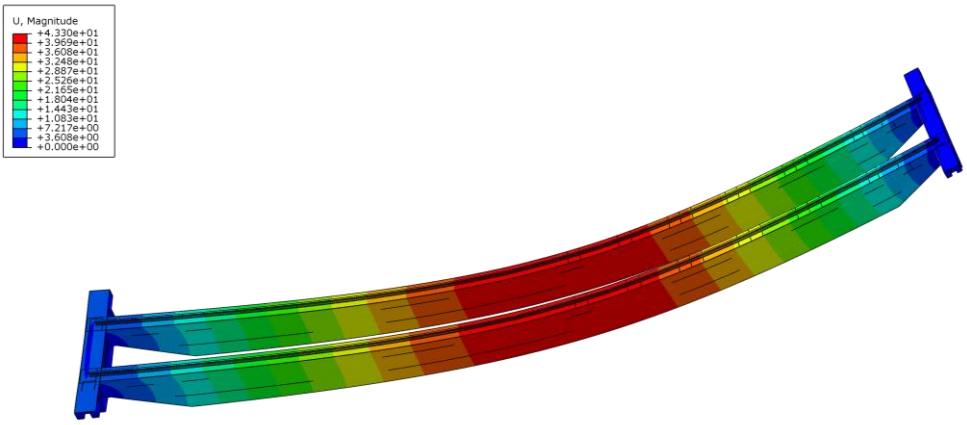

Figure 7. Equivalent displacement nephogram of trolley with full loaded in 1/2 cross girder.

Table 2. Stress and displacement of the girder.

Load conditions	Maximum stress [MPa]	Maximum stress position	Maximum displacement [mm]	Maximum displacement position
In the middle of the girder	120.4	Where the load is applied and the middle of lower cover	43.3	The middle of the web
At 1/4 of the girder	112.4	Where the load is applied and the middle of lower cover	33.2	The middle of the web
At the end ofthe girder	119	The end of the upper cover	17.5	The middle of the web

Calibrate the strength and stiffness of the girder when the travelling crab is in the mid-span position.

The girder material is Q235 steel, and its Yield strength $\sigma_s = 235MPa$. Take the safety factor as $n_s = 1.33$, and $\sigma_{\max} = 120.4MPa$.

Allowable stress:

$$[\sigma] = \frac{\sigma_s}{n_s} = 176.7MPa \quad (1)$$

Strength conditions:

$$\sigma_{\max} = 120.4 < [\sigma] = 176.7 \quad (2)$$

Therefore, the strength of the crane main girder meets the design requirement

The span of the crane is 31500mm, and the maximum displacement $u_{\max} = 43.3(mm)$.

$$u_{\max} = 43.3 \le \frac{1}{700} S = 45 \quad (3)$$

Therefore, the stiffness of the crane main girder meets the design requirements.

4 Theoretical calculation

In order to verify the accuracy of the finite element analysis results, the following theoretical calculations are performed on the stress and displacement of the main beam.

4.1 Main girder loading situation

Loads in the vertical plane:

Main beam weight $G = 163856(N)$, and the weight evenly distributed to the girder is $q = \frac{G}{31.5} = 5202(N/m)$.

trolley weight $P = 153860(N)$

Working load $Q = 490000(N)$

Calculated load $Q_1 = Q_2 = \frac{P + Q\phi_2}{4} = 178115N$

Loads in the horizontal plane: Inertia force during crane operation $q_0 = \frac{G}{g} \cdot a = 4846(N)$,Where acceleration $a = 0.32(m/s^2)$.

The loading of the main girder in the vertical and horizontal planes is shown in Fig 8 and Fig 9.

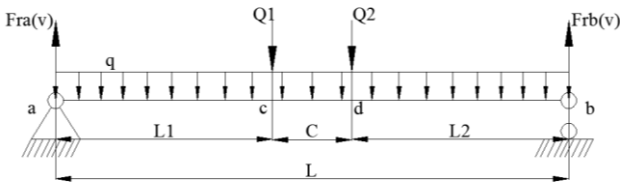

Figure 8. Loads in the vertical plane.

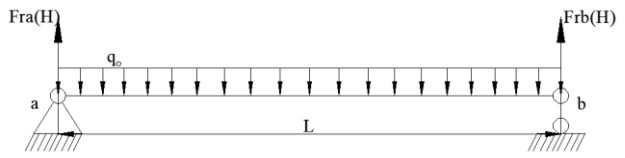

Figure 9. Loads in the horizontal plane.

4.2 Main girder section

For the convenience of calculation, the main girder is treated as an equal section, and its structural dimensions are shown in Fig 10.

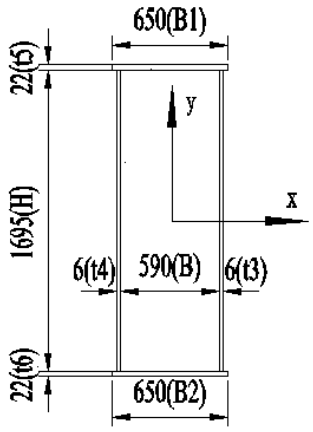

Figure 10. Main girder section.

4.3 The shear and bending moments of the vertical plane

Inertia moments I_x, I_y.

$$I_{x上} = I_{x下} = \frac{B_1 t_5^3}{12} + \left(\frac{H}{2}\right)^2 \cdot B_1 t_5$$

$$I_{x左} = I_{x右} = \frac{t_4 H^3}{12}$$

$$I_{y上} = I_{y下} = \frac{t_4 H^3}{12}$$

$$I_{y左} = I_{Y右} = \frac{H t_4^3}{12} + \left(\frac{B}{2}\right)^2 \cdot t_4 H$$

$$I_x = 2I_{x上} + 2I_{x左} = 28.1 \times 10^{-3}(m^4)$$

$$I_y = 2I_{y下} + 2I_{y右} = 2.91 \times 10^{-3}(m^4)$$

Bending section coefficient W_x, W_y.

$$W_x = \frac{I_x}{y_{\max}} = 33.16 \times 10^{-3}(m^3)$$

$$W_y = \frac{I_y}{x_{\max}} = 9.86 \times 10^{-3}(m^3)$$

Vertical surface reaction force $F_{ra}{}^V$, $F_{rb}{}^V$.

Balance condition:

$$\sum M_B = F_{ra}{}^V L - \frac{1}{2} qL^2 - Q_1(C + L_2) - Q_2 L_2 = 0$$

$$\sum Y = F_{ra}{}^V + F_{rb}{}^V - qL - Q_1 - Q_2 = 0$$

Where $L = 31.5(m)$, $C = 3.58(m)$, $L_2 = 13.96(m)$, $Q_1 = Q_2 = 177237.5(N)$, $q = 5202(N/m)$, and get $F_{ra}{}^V = F_{rb}{}^V = 259169(N)$.

Shear force $F(x)$.

Part a-c, $F(x) = F_{ra}{}^V - qx$, $0 \le x \le 13.96$

Part b-d, $F(x) = F_{ra}{}^V - qx - Q_1$, $13.96 \le x \le 17.54$

Part c-b, $F(x) = F_{ra}{}^V - qx - Q_1 - Q_2$, $17.54 \le x \le 31.5$

Maximum shear $F_{\max} = 259165.72(N)$.

Fig 11 shows the main girder vertical shear diagram.

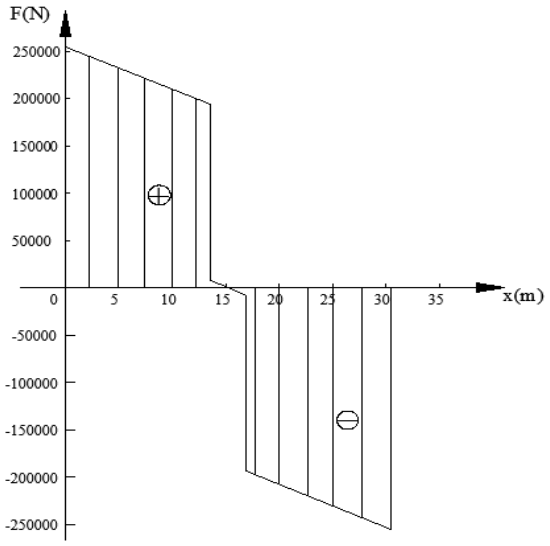

Figure 11. Main girder vertical shear diagram.

Bending moment $M(x)$.

Part a-c, $M(x)=F_{ra}{}^{V}x-\frac{1}{2}qx^{2},0\le x\le 13.96$

Part b-d,

$$M(x)=F_{ra}{}^{V}x-\frac{1}{2}qx^{2}-Q_{1}(x-13.96),13.96\le x\le 17.54$$

Part c-b,

$$M(x)=F_{ra}{}^{V}x-\frac{1}{2}qx^{2}-Q_{1}(x-13.96)-Q_{2}(x-17.54),$$

$$17.54\le x\le 31.5$$

Maximum bending moment

$M_{\max}{}^{V}=3111086.9(N\cdot m)$.

Fig 12 shows the main girder vertical bending moment diagram.

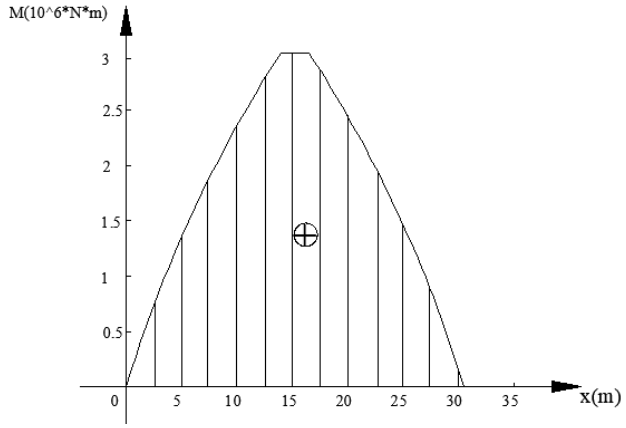

Figure 12. Main girder vertical bending moment diagram.

4.4 The shear and bending moments of the horizontal plane

Maximum shear and bending moments can be obtained in the same way as in Section 4.3.

Maximum shear $F_{\max}=2423(N)$

Maximum bending moment $M_{\max}{}^{H}=19081.3(N\cdot m)$

4.5 Calculation of maximum stress and displacement

Maximum bending normal stress

$$\sigma=\frac{M_{\max}{}^{V}}{W_x}+\frac{M_{\max}{}^{H}}{W_y}=116.2(MPa)$$

Maximum shear stress $\tau=\frac{F_{\max}S^{*}}{2I_x t_4}=13.62(MPa)$

Comprehensive stress $\sigma_{\max}=\sqrt{\sigma^{2}+3\tau^{2}}=118.6(MPa)$

Displacement of the main beam in the vertical direction $f=\frac{(1.1G_{小车}+1.14Q)L^{3}}{2\times 48EI_x}=42.3(\mathrm{mm})$.

5 Summary

In this paper, the finite element analysis of QD-type (50/10t-31.5) hooked bridge crane metal structure was carried out using ABAQUS software. Through the comparison of three different working conditions, it can be seen that the stress and displacement of the girder is maximum when trolley with full loaded in 1/2 cross girder. The maximum stress $\sigma_{\max}=120.4MPa$, and the maximum displacement $u_{\max}=43.3mm$. It is obvious that it meets the design requirements and has a certain amount of margin. Moreover, the maximum stress and displacement under dangerous conditions of the crane are calculated by theoretical calculation. By comparing the results of the theoretical method and the finite element method, we find that the finite element calculation model has good precision.

References

1. Tang R, Huang J, Control of bridge cranes with distributed-mass payloads under windy conditions, Mechanical Systems & Signal Processing, **72-73**(2016):409-419.
2. Liu B, Zhang Q, Xing J X, Design of Bridge Crane Metal Structure Based on Limit State Design Method, Mechanical Engineering & Automation, **3**(2011):031.
3. Jiong G, Weichen Y, Research on crane rapid customization design system, Hoisting and Conveying Machinery, **2**(2014): 015.
4. Tong Y, Tang Z, Ye W, Yang Z, Research on energy-saving optimization design of bridge crane, Polskie Naukowo-Techniczne Towarzystwo Eksploatacyjne, **15**(2013):449-457.
5. GUAN Z, ZHANG Q, GUO J, The Finite Element Analysis of QD250/50/10t-25.5 Bridge Crane, Journal of Shanghai Electric Technology, **2**(2011): 004.
6. Kloosterman G, Bouwman V, Automatic remeshing and rezoning for the simulation of 3D glass bottle forming with Abaqus/CAE, Abaqus/Standard and Abaqus/Explicit, International Journal of Material Forming, 2(2009):105-108.